J Electroceram (2008) 20:259–264
DOI 10.1007/s10832-007-9190-7

Actuation performance analysis of piezo-composite unimorph actuator with d_{33} actuation mechanism of piezo-electric ceramic layer

Anh Kim Tran · Nam Seo Goo · Kwang Joon Yoon

Received: 21 2007 / Accepted: 25 June 2007 / Published online: 1 August 2007

Abstract The performance improvement of the LIPCA (Lightweight Piezo-Composite curved Actuator) is investigated in this paper. The LIPCA is known as the best layered piezo-composite unimorph actuator because of not only high performance but also its flexible analytical design model and simple fabrication technique. Besides, originated from efforts to develop highly induced-strain piezoelectric ceramic, the IDEAL (Inter-Digitated Electrode Actuation Layer) have shown to be a potential candidate in unimorph or bimorph actuator designs. In a latest model of IDEAL designs, the inter-digitated electrodes (IDEs) had been proposed to be embedded directly into the piezoelectric ceramic wafer. Hence, the resulting stacked-type transducer is able to have full d_{33} actuation mechanism which can produce almost twice larger strain than that produced by the conventional d_{31} actuation mechanism. Therefore, by replacing the original actuation layer with IDEAL in the lay-up structure of the conventional LIPCA design, one can expect improvement to the performance of the actuator, e.g., gaining higher of out-of-plane actuation displacement. The modified design of LIPCA had been investigated considering mechanical properties of an inhomogeneous IDEAL. As the result, an IDEAL fabricated with low-elastic-modulus IDEs have shown to give considerably improvement on actuation performance of the LIPCA. Following that sense, a new homogenization model applied to the embedded IDEAL is proposed and able to convince the previously obtained result.

A. K. Tran · N. S. Goo · K. J. Yoon (✉)
Artificial Muscle Research Center, Department of Advanced Technology Fusion, Konkuk University,
Seoul 143-701, South Korea
e-mail: kjyoon@konkuk.ac.kr

Keywords Unimorph · PZT · LIPCA · IDEAL · Homogenization

1 Introduction

Nowadays, many actuators are employing piezoelectric ceramics as the basis transducers. Among those piezoelectric ceramic based actuators, the terms like "unimorph", "bimorph" are the most familiar ones. Due to a couple of technical reasons, "unimorph" is much preferred to its "bimorph"-sister. Particularly, THUNDER (Thin UNimorph DrivER), RAINBOW (Reduced And Internally Biased Oxide Wafer) and LIPCA [1–3] are among the most famous actuators found in the "unimorph" family. Moreover, even properties of each of these actuators can make them appropriate in certain opposite applications, many advantages of LIPCA such as design flexibility, light weight, ease of manufacturing... have all contributed to make this actuator become a potential candidate in various applications. It is clear that, the most important criterion of an actuator is the capability to produce a high displacement. In a unimorph actuator design, in general, when the actuation layer is placed apart from the flexural neutral surface of the lay-up structure, i.e., at a certain moment arm, the induced force functions in forming a bending moment. In responding to that applied moment, the actuator arches and ends up at a certain out-of-plane displacement. According to an analytical formulation for the design process of LIPCA, a properly changing in the lay-up structure is among ways to obtain a greater moment arm [4]. Similarly, by concurrently adjusting the bending stiffness as well as properties of the active layer one might expect improvement on actuation performance. Therefore, conducting parametric study specifically for the actuation layer might be helpful to

determine a configuration which is able to enhance the actuation performance of the actuator. By following this way, one can get benefit from previous studies which related to improvement of extensional-mode transducers. Among previous extensional-mode piezoelectric transducers, designs that follow d_{33} actuation mechanism are of much interest since those ones are capable to induce comparatively larger strain than that actuated through d_{31} mechanism [5]. To incorporate the d_{33} actuation mechanism, the Active Fiber Composites Actuator (AFCs) was first developed at the Active Material and Structure Lab. of MIT [6] and the Macro Fiber Composites Actuator (LaRC-MFCTM) was developed at the NASA Langley Research Center [7]; the IDEAL was developed at Artificial Muscle Research Center of Konkuk University [8, 9].

In one of our recently studies, it was shown that different design of IDEALs could improve the performance of LIPCA [9]. In that work, the embedded IDEAL was refereed to as an electro-active layer in the design of the LIPCA which have been investigated parametrically. As the result, actuation performance of the LIPCA had been improved quite considerably when employing the embedded IDEAL whose electrode made of a low-elastic modulus material.

Moreover, as a non-homogeneous material, the embedded IDEAL still needs a more reliable homogenization model in order to convince the obtained result. Therefore, in this paper, another homogenization model is employed to estimate effective mechanical properties of the embedded IDEAL. Those effective properties are then served for the analytical design model developed before in order to investigate the performance of the actuator. Influences of the different design of IDEALs on the LIPCA's performance and correlation with previously obtained result are also investigated.

2 Analysis

2.1 Effective mechanical properties of the embedded IDEAL

Since the embedded IDEAL has a two-media regulated structure, there is need to estimate equivalent quantities of this non-homogeneous solid. Unlike what had been shown in our previous work [9], formulation presented here relies on powerful capabilities of commercial Finite Element Analysis package like MSC Patran/Nastran. That is, one can virtually apply a simple loading condition to the model and easily obtain the physical response data. For simplicity, the equivalent quantities including effective elastic moduli, coefficients of thermal expansion (CTEs) are estimated basing upon an idealized 2D orthotropic solid model where both piezoelectric ceramic and electrode constituents are arranged on a 2D plane and followed a plane-stress constitutive governing equation (Fig. 1):

$$\begin{Bmatrix} \overline{\sigma}_{11} \\ \overline{\sigma}_{22} \\ \overline{\sigma}_{12} \end{Bmatrix} = \begin{bmatrix} \frac{E_1}{1-\nu_{12}\nu_{21}} & \frac{\nu_{12}E_2}{1-\nu_{12}\nu_{21}} & 0 \\ \frac{\nu_{12}E_2}{1-\nu_{12}\nu_{21}} & \frac{E_2}{1-\nu_{12}\nu_{21}} & 0 \\ 0 & 0 & G_{12} \end{bmatrix} \begin{Bmatrix} \overline{\varepsilon}_{11} - \Delta T \cdot \overline{\alpha}_1 \\ \overline{\varepsilon}_{22} - \Delta T \cdot \overline{\alpha}_2 \\ \overline{\gamma}_{12} \end{Bmatrix} \tag{1.a}$$

$$\begin{Bmatrix} \overline{\varepsilon}_{11} - \Delta T \cdot \overline{\alpha}_1 \\ \overline{\varepsilon}_{22} - \Delta T \cdot \overline{\alpha}_2 \\ \overline{\gamma}_{12} \end{Bmatrix} = \begin{bmatrix} \frac{1}{E_1} & \frac{-\nu_{12}}{E_1} & 0 \\ \frac{-\nu_{12}}{E_1} & \frac{1}{E_2} & 0 \\ 0 & 0 & \frac{1}{G_{12}} \end{bmatrix} \begin{Bmatrix} \overline{\sigma}_{11} \\ \overline{\sigma}_{22} \\ \overline{\sigma}_{12} \end{Bmatrix} \tag{1.b}$$

As shown in the Fig. 1, the subscript notation f indicates the ceramic media while m refers to the electrode constituent. For convenient, a whole wafer is chosen as a representative volume element (RVE). Therefore, the percentage ratios c_f, c_m for the constituents are calculated as following:

$$c_f = \frac{n_{ce} l_{ce}}{n_{ce} l_{ce} + n_{el} l_{el}}; \quad c_m = \frac{n_{el} l_{el}}{n_{ce} l_{ce} + n_{el} l_{el}} \tag{2}$$

where l_{ce}, n_{ce} are length of each piezoelectric ceramic solid in the stacking direction and number of stacking components respectively. l_{el}, n_{el} are individual length of inter-digitated electrodes and number of electrode gaps between stacking piezoelectric ceramic solids.

There are two assumptions imposed for the RVE, e.g., a constant strain assumption (Voigt model) applied in the ceramic fiber direction and a constant stress assumption (Reuss model) validated for the in-plane stresses [10]:

$$\varepsilon^{f}_{11} = \varepsilon^{m}_{11} = \overline{\varepsilon}_{11} \tag{3.a}$$

$$\sigma^{f}_{12} = \sigma^{m}_{12} = \overline{\sigma}_{12} \tag{3.b}$$

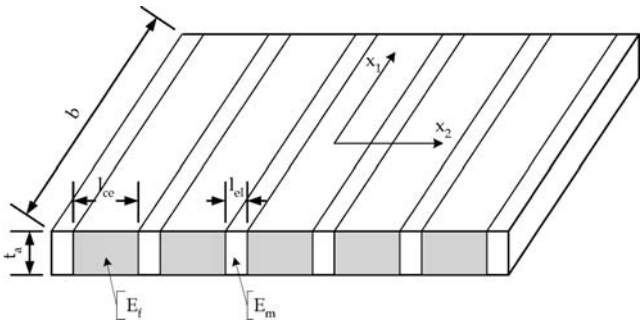

Fig. 1 An idealized 2D model of the embedded inter-digitated electrode actuation layer

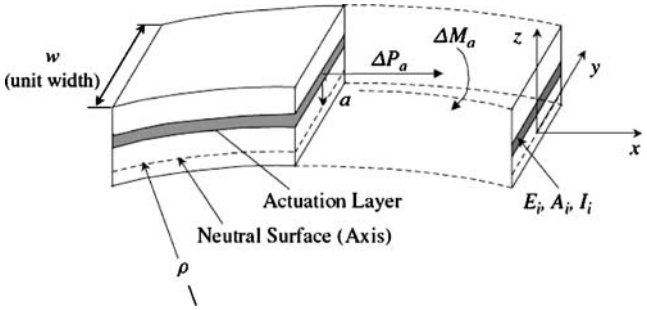

Fig. 2 Schematic for the curvature change of a laminated beam with an electro-active layer

By considering both stress and strain are constant in each constituent, the average stress and strain of the RVE obey the following relations:

$$\overline{\sigma}_{11} = c_f \sigma^f_{11} + c_m \sigma^m_{11} \tag{4.a}$$

$$\overline{\sigma}_{22} = c_f \sigma^f_{22} + c_m \sigma^m_{22} \tag{4.b}$$

$$\overline{\varepsilon}_{22} = c_f \varepsilon^f_{22} + c_m \varepsilon^m_{22} \tag{4.c}$$

$$\overline{\gamma}_{12} = c_f \gamma^f_{12} + c_m \gamma^m_{12} \tag{4.d}$$

Following the methodology given elsewhere, one can estimate equivalent quantities as the followings [10]:

1. When the RVE is loaded in the fiber direction, (x_1 direction), one can assume:

$$\overline{\sigma}_{11} \neq 0, \quad \overline{\sigma}_{22} = \overline{\sigma}_{12} = 0 \tag{5}$$

$$E_1 = \frac{\left(c_f \sigma^f_{11} + c_m \sigma^m_{11}\right)\left(c_f E_f + c_m E_m\right)}{c_f\left(\sigma^f_{11} - \nu_f \sigma^f_{22}\right) + c_m\left(\sigma^m_{11} - \nu_m \sigma^m_{22}\right)} \tag{6.a}$$

$$\nu_{12} = \frac{-\left(c_f E_f + c_m E_m\right)\left(\frac{c_f}{E_f}\left(\sigma^f_{22} - \nu_f \sigma^f_{11}\right) + \frac{c_m}{E_m}\left(\sigma^m_{22} - \nu_m \sigma^m_{11}\right)\right)}{c_f\left(\sigma^f_{11} - \nu_f \sigma^f_{22}\right) + c_m\left(\sigma^m_{11} - \nu_m \sigma^m_{22}\right)} \tag{6.b}$$

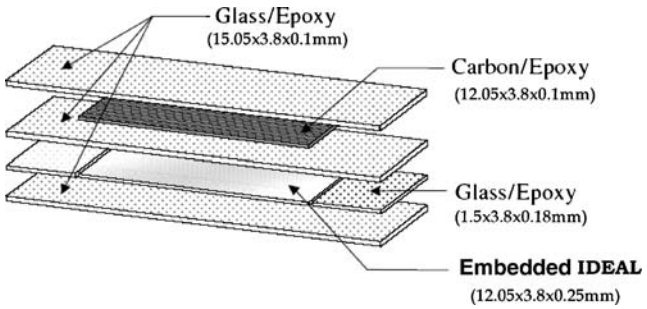

Fig. 3 Geometry of mini-LIPCA [9]

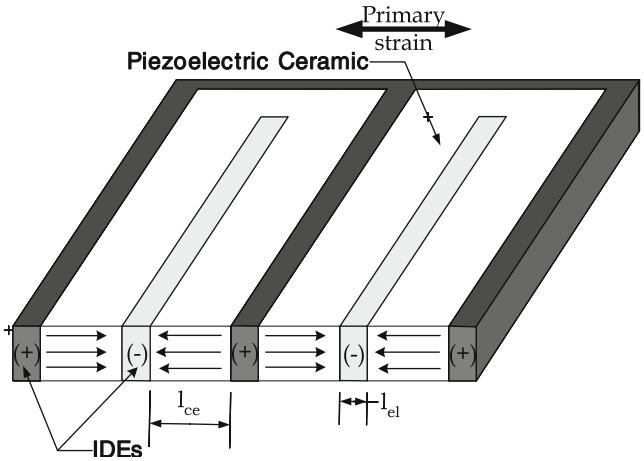

Fig. 4 Schematic feature of the embedded IDEAL

where σ^f_{11}, σ^f_{22}, σ^m_{11}, σ^m_{22} are average stress components in piezoelectric ceramic and in electrode medium. Those quantities can be estimated using Nastran/Patran software which can give reliable solution based on a finite element analysis model of RVE with given loading condition (Eq. 5).

2. When the RVE is under a pure-shear load:

$$\overline{\sigma}_{12} \neq 0, \quad \overline{\sigma}_{11} = \overline{\sigma}_{22} = 0 \tag{7}$$

then

$$\frac{1}{G_{12}} = \frac{c_f}{G_f} + \frac{c_m}{G_m} \tag{8}$$

3. By applying a uniformly pulling force on the RVE along the y direction, after all, one can estimate an effective modulus E_2 as follows:

$$E_2 = \frac{c_f \sigma^f_{22} + c_m \sigma^m_{22}}{\left(\frac{c_f}{E_f}\sigma^f_{22} + \left(\frac{c_f \nu_{12}}{E_1} - \frac{c_f \nu_f}{E_f}\right)\sigma^f_{11}\right) + \left(\frac{c_m}{E_m}\sigma^m_{22} + \left(\frac{c_m \nu_{12}}{E_1} - \frac{c_m \nu_m}{E_m}\right)\sigma^m_{11}\right)} \tag{9}$$

Similar to the model using to estimate E_1 and ν_{12}, a new loading condition should be applied again on this model in order to obtain a new set of σ^f_{11}, σ^f_{22}, σ^m_{11}, σ^m_{22} for the estimation of E_2 in (Eq. 9).

4. Considering the piezoelectric ceramic has different in-plane CTEs α^f_1, α^f_2 and the electrode constituent material has an in-plane isotropic CTE α^m. During thermal expansion or contraction, if there is no applied load to constrain the displacement, then the RVE should be stress-free. So, equivalent thermal coefficients are calculated as following:

$$\overline{\alpha}_1 = \frac{c_f E_f \alpha^f_1 + c_m E_m \alpha^m}{c_f E_f + c_m E_m} \tag{10.a}$$

$$\overline{\alpha}_2 = c_f\left(\alpha^f_2 + \nu_f \alpha^f_1\right) + c_m \alpha^m (1 + \nu_m) - \left(c_f \nu_f + c_m \nu_m\right)\overline{\alpha}_1 \tag{10.b}$$

Table 1 Basic properties of actuator materials.

Properties		Piezoelectric ceramic	Carbon/epoxy	Glass/epoxy	Aluminium	Gold	Conductive epoxy
Modulus	E_1 (GPa)	62	231.2	21.7	70	77	2.5
	E_2 (GPa)	62	7.2	21.7	70	77	2.5
	G_{12} (GPa)	23.66	4.3	3.99	25.93	26.74	0.89
	v_{12}	0.31	0.29	0.13	0.35	0.44	0.4
CTE	α_1 (10^{-6} K^{-1})	3.5	−1.58	14.2	23.1	14.2	45
	α_2 (10^{-6} K^{-1})	3.5	32.2	14.2	23.1	14.2	45
Piezoelectric strain coefficients d_{31}, d_{33} (10^{-12} mV^{-1})		−320, 650	–	–			
Thickness	t (mm)	0.25	0.1	0.09	0.05	0.05	0.05

Once finishing the estimation of equivalent quantities as shown in Eqs. 6.a–b, 8–9, 10.a–b, one can consider the RVE of the embedded IDEAL as a homogeneous solid. An analytical model of LIPCA having the embedded IDEAL can employ those equivalent moduli to investigate a curing or thermal exciting process. This content will be discussed further in Section 2 where a non-homogeneous active layer is included in an analytical design model.

2.2 Analytical design model

As having been explained in our previous works [4, 9], a high performance unimorph actuator like LIPCA should be capable to produce a large bending moment while owning a moderate bending stiffness. Formulation is briefly presented here for reader's convenience. That is, for an actuator having unit width the change in the curvature can be expressed as follows:

$$\Delta\kappa = \frac{1}{\Delta\rho} = \frac{\Delta M_a}{D} \tag{11}$$

where D is the total bending stiffness which is the total of bending stiffness of each layer.:

$$D = \sum_k (E_i I_i) = \sum_k \left(\int_{z_{k-1}}^{z_k} E_i (z - z_n)^2 dz \right)$$

$$= \sum_k \left(E_i \frac{(z - z_n)^3}{3} \Big|_{z_{k-1}}^{z} \right) \tag{12}$$

where the neural surface position z_n is a solution of the following equation [11]:

$$\sum_k \left(\int_{z_{k-1}}^{z_k} E_i \frac{(z - z_n)}{\rho} \, dz \right) = 0 \tag{13}$$

Once there is a non-homogeneous layer, its equivalent elastic modulus E_i is taken into account in Eqs. 12–13. Also, ΔM_a is the sum of two components:

$$\Delta M_a = \Delta M_a^{ce} + \Delta M_a^{el} \tag{14}$$

where ΔM_a^{ce} is the induced bending moment generated by applied electric field $\frac{\Delta V}{l_{ce}}$ and ΔM_a^{el} is the secondary bending

Table 2 Effective moduli calculated by different homogenization formulation.

Effective properties		Embedded IDEAL fabricated with electrode		
		Al	Au	Conductive Epoxy
E_1 (GPa)		68.21 (63.31)	70.01 (64.5)	54.68 (52.45)
E_2 (GPa)		64.02 (63.18)	65.03 (64.06)	27.23 (18.54)
G_{12} (GPa)		24 (24)	24.11 (24.11)	5.96 (5.96)
v_{12}		0.096 (0.31)	0.1 (0.33)	0.057 (0.32)
CTE	α_1 (10^{-6} K^{-1})	7.04 (7.04)	5.6 (5.6)	3.95 (3.95)
	α_2 (10^{-6} K^{-1})	6.7 (6.7)	5.32 (5.32)	12.84 (12.84)

( ): Calculated data in [9].

Table 3 Analytical design parameters of LIPCA with different electro-active layers.

Mini-LIPCA with active-layer made of		Bending stiffness (D 10^{-2} Nm^{-2})	Moment arm a (10^{-4} m)	$c_{ua}=a$ / D (10^{-2} N^{-1} m^{-1})	Induced bending moment ΔM_a (10^{-5} Nm)	Curvature $\left(\Delta\kappa=\frac{\Delta M_a}{D}\right)$ (10^{-2} m^{-1})
PZT-d31 (t_a=0.25 mm) Embedded IDEAL (l_{ce}=0.25 mm)		0.4	1.536	3.87	1.16*ΔV (*)	0.29*ΔV(*)
Electrode (l_{el}=0.05 mm)	Al	0.4	1.5254	3.79	1.955*ΔV(**)	0.486*ΔV(**)
	Au	0.41	1.5179	3.74	1.953*ΔV(**)	0.482*ΔV(**)
	Cond. Epx.	0.28	2.0318	7.13	2.69*ΔV(**)	0.95*ΔV(**)

*, **: the d_{31} mechanism causes bending in opposite direction to which driven by d_{33} mechanism

moment caused by strain induced in the electrode constituent. The ΔM_a^{el} is calculated by taking a product of induced force $\Delta P_a^{ce} = t_a E_a^{ce} \varepsilon_{11}^{ce}$ and the moment arm a. In this paper, the active wafer is considered to be excited via d_{33} actuation mechanism. In the scalar form, ΔM_a^{ce} is formulated as following:

$$\Delta M_a^{ce} = a t_a E_a^{ce} d_{33} \frac{\Delta V}{l_{ce}} \tag{15}$$

where t_a is the thickness of the active wafer, E_a^{ce} is the elastic modulus of the piezoelectric ceramic.

Similarly, ΔM_a^{el} can be calculated as following:

$$\Delta M_a^{el} = a t_a E_a^{el} \varepsilon_{11}^{el} \tag{16}$$

Since $l_{ce} \gg l_{el}$ and ε_{11}^{el} is small enough as a result of its constraint to the upper and lower sandwiched layers, therefore one can neglect the second part of the right hand side of Eq. 14, hence:

$$\Delta M_a \approx \Delta M_a^{ce} = a t_a E_a^{ce} d_{33} \frac{\Delta V}{l_{ce}} \tag{17}$$

Then the change in curvature of the laminated beam is expressed as following:

$$\Delta\kappa = \frac{\Delta M_a}{D} = \frac{a}{D} t_a E_a^{ce} \frac{d_{33}}{l_{ce}} \Delta V = c_{ua} t_a E_a^{ce} d_{33} \frac{\Delta V}{l_{ce}} \tag{18}$$

Therefore, by trying to reduce D in Eq. 12 and also increase the moment arm a with a new solution of z_n in Eq. 13, considerable increment of the curvature $\Delta\kappa$ is expected. Hence, performance of the actuator would be improved substantially (Fig. 2).

3 Comparison of actuator performances

Based upon the conventional design of LIPCA, a new Mini-LIPCA has been designed [9]. As shown in the Fig. 3, the new LIPCA is scaled down and actuated by the embedded IDEAL. Unlike the conventional design, the electro-active layer in this new LIPCA is excited though d_{33} actuation mechanism which can induce higher strain than that induced by the old wafer with d_{31} mechanism.

As explained in [8], the embedded IDEAL was proposed to be fabricated using MEMS (Micro-Electro Mechanical System) technology. The IDEs are electroplated directly into the piezoelectric ceramic by replacing the portion of the ceramic material which had been etched away. Schematically, the transducer is illustrated as shown in the Fig. 4.

According to the fabrication process of the embedded IDEAL, alternative conductive materials can be designated as the electrode of the transducer. This variation have shown to impact to the performance of the LIPCA. Three electrode candidates are selected to investigate this phenomenon, e.g. aluminum, gold, and conductive epoxy. The properties of all concerned materials are listed in the Table 1. Table 2 shows comparison between equivalent properties of the embedded IDEAL calculated by current and previous work [9] which have been mentioned in Section 2.1. For comparison purpose, in Table 3., c_{ua} and the moment arm a of the actuator with respect to each electrode have been calculated according to the formulas given in Section 2. We found that the prediction values for the curvature change are quite close to the results predicted in our previous work, e.g., the embedded IDEAL with conductive electrodes gave the largest bending curvature to the LIPCA [9].

4 Conclusions

The present paper has shown the investigation of performance of LIPCA with embedded IDEAL as an electro-active layer. Based upon the conventional LIPCA design, the actuator was proposed to employ the embedded IDEAL as a substitution to the original actuation layer which has d_{31} actuation mechanism. This embedded IDEAL is known as a stacked type actuator which can achieve full d_{33} actuation mechanism. Since the d_{33} actuation mechanism can produce higher strain than d_{31}, a higher performance

could be expected. The investigation has been performed by assuming the embedded IDEAL can be fabricated with alternative embedded electrodes and each of which has different material properties. Besides, a new homogenization model is proposed to find effective mechanical properties of the inhomogeneous embedded IDEAL. The differences of material properties of electrode eventually affect to the performance of the LIPCAs. That is, the actuation displacement of LIPCA can be increased considerably once employing the embedded IDEAL whose electrodes made of a low-elastic-modulus material. The finally obtained results agree well with what had been obtained in our last work where a different homogenization model had been applied.

Acknowledgment This work was supported by the grants from Intensive Research Center Program of the Korea Research Foundation (KRF-2004-005-D00045-7). The authors acknowledge the support.

References

1. Y.K. Joon, P.H. Chul, Curved shape actuator device composed of electro active layer and fiber composite layers, US Patent No. 7,081,701 B2, 2006.7.25
2. K.M. Mossi, R.P. Bishop. Characterization of different types of high performance THUNDER actuators, SPIE's conference proceeding, Newport Beach, CA (1999)
3. G.H. Haertling, RAINBOW actuators and sensors: a new smart technology, Proceeding of SPIE Conference, San Diego, CA (1997)
4. K.J. Yoon, K.H. Park, S.K. Lee, N.S. Goo, H.C. Park, Analytical design model for a piezo-composite unimorph actuator and its verification using lightweight piezo-composite curved actuators, Smart Mater. Struct. **13**, 459 (2004)
5. M.-S. Choi, Improvement of the design method using the KLM model for optimizing thickness-mode piezoelectric transducers, J. Korean Phys. Soc. **45**, 1517 (2004)
6. A.A. Bent, Active fiber composite material systems for structural control applications, SPIE's 6th International Symposium on Smart Structures and Materials, Newport Beach, CA (1999)
7. W.K. Wilkie, et al., Low-cost piezocomposite actuator for structural control applications, SPIE's 7th Annual International Symposium on Smart Structures and Materials, Newport Beach, CA (2000)
8. Y.K. Joon, Y.Y. Soo, P.H. Chul, G.N. Seo, Electro active material actuator embedded with interdigitated electrodes, International App. No. PCT/KR2005/003417, 2005.10.13
9. A.K. Tran, N.S. Goo, K.J. Yoon, Actuation performance improvement of lightweight piezo-composite curved actuator with an interdigitated electrode actuation layer, J. Korean Phys. Soc. (2006)
10. R.M. Jones, *Mechanics of Composite Materials*, 2nd edn. (Taylor & Francis, 1999)
11. X. Li, W.Y. Shih, I.A. Aksay, W.-H. Shih, Electromechanical behavior of PZT-brass unimorphs, J. Am. Ceram. Soc. **82**, 1733 (1999)